Pitfalls in the Staging of Cancer of the Major Salivary Gland Neoplasms

Elliott R. Friedman, MD[a,*], Amit M. Saindane, MD[b]

KEYWORDS

• Salivary glands • Adenoid cystic carcinoma • Benign mixed tumor
• Carcinoma ex pleomorphic adenoma

KEY POINTS

- The major salivary glands consist of the parotid, submandibular, and sublingual glands.
- Most neoplasms in other subsites in the head and neck are squamous cell carcinoma, but tumors of the salivary glands may be benign or malignant.
- Surgical treatment differs if the lesion is benign, and therefore preoperative fine-needle aspiration is important in salivary neoplasms.
- The role of imaging is to attempt to determine histology, predict likelihood of a lesion being malignant, and report an imaging stage.
- This article reviews the various histologies, imaging features, and staging of major salivary gland neoplasms.

ANATOMY AND BOUNDARIES

The major salivary glands consist of the parotid, submandibular, and sublingual glands. Submucosal clusters of salivary tissue located in the palate, oral cavity, paranasal sinuses, and upper aerodigestive tract are minor salivary glands, and are variable in distribution. Primary neoplasms arising in the minor salivary glands are staged according to the anatomic site of origin.[1]

The parotid gland is the largest of the salivary glands, the bulk of which lies superficial to the masseter muscle and mandibular ramus and angle (**Fig. 1**). The investing fascia arises from the superficial layer of the deep cervical fascia. The deep portion of the gland extends through the stylomandibular tunnel into the prestyloid compartment of the parapharyngeal space. The stylomandibular tunnel is formed by the skull base, posterior margin of the mandibular ramus, and styloid process and stylomandibular ligament.[2] Although the parotid gland is a single contiguous structure, for surgical convenience it has been divided into superficial and deep lobes by the course of the facial nerve, which courses lateral to the retromandibular vein. Most neoplasms arise in the superficial portion of the gland.[3] Considerable variation in intraparotid facial nerve anatomy exists, but most commonly the nerve enters the posteromedial aspect of the gland and divides into 2 main trunks before dividing into 5 main branches: temporal, zygomatic, buccal, mandibular, and cervical. The auriculotemporal nerve, which curves around the mandibular neck, embedded in the gland capsule, connects the mandibular branch of the trigeminal nerve with the facial nerve and serves as a potential route of perineural tumor spread.

Accessory parotid tissue is found in approximately 20% of the population, anterior to the parotid gland, typically overlying the masseter muscle between the zygomatic arch and parotid

[a] Department of Diagnostic & Interventional Imaging, University of Texas Health Science Center at Houston, 6431 Fannin Street, MSB 2.130B, Houston, TX 77030, USA; [b] Department of Radiology and Imaging Sciences, Emory University School of Medicine, BG-22, 1364 Clifton Road Northeast, Atlanta, GA 30322, USA
* Corresponding author.
E-mail address: Elliott.Friedman@uth.tmc.edu

Neuroimag Clin N Am 23 (2013) 107–122
http://dx.doi.org/10.1016/j.nic.2012.08.009
1052-5149/13/$ – see front matter

Fig. 1. CT anatomy of the parotid gland. *Abbreviations:* m, muscle; n, nerve; v, vein.

duct.[4] In distinction to other salivary glands, between 3 and 24 lymph nodes are found within the parotid gland, almost all within the superficial portion of the gland.[5] Parotid lymph nodes drain into the level IIA and IIB upper cervical chains.[2] The main parotid duct, Stensen's duct, is approximately 7 cm in length, exiting the anterior aspect of the gland, passing horizontally lateral to the masseter muscle and medial to the zygomaticus major muscle, pierces the buccinator muscle, and opens on a papilla in the buccal mucosa opposite the second maxillary molar tooth.[4]

The submandibular gland occupies most of the submandibular triangle, which is formed by the inferior border of the mandibular body and anterior and posterior bellies of the digastric muscle (**Fig. 2**). The stylohyoid muscle also forms part of the posterior boundary. The submandibular gland is enveloped by a thin fibrous capsule. The stylomandibular ligament, a reflection of the deep cervical fascia, separates the parotid and submandibular glands. The submandibular gland is arbitrarily divided into superficial and deep lobes based on its extension around the posterior margin of the mylohyoid muscle, which divides the submandibular space from the floor of the mouth. No lymph nodes or large nerves are present within the submandibular gland. Lymphatic drainage is into IB or submandibular nodes and deep cervical lymph nodes, particularly IIA nodes. Wharton's duct, the primary excretory duct, courses anteriorly and superiorly between the genioglossus muscle and sublingual gland to open in the floor of mouth on the sublingual papilla on the side of the tongue.[4]

The anterior facial vein, which runs along the lateral margin of the submandibular gland, can be used to distinguish exophytic submandibular masses from extrinsic lesions, such as lymphadenopathy or soft tissue tumors, that arise adjacent to the gland. A mass separated by the facial vein from the gland must be an extrinsic lesion.[6]

The sublingual gland is the smallest of the major salivary glands and is situated above the mylohyoid muscle, covered by mucosa of the floor of the mouth.[4] No well-defined capsule exists. Numerous small excretory ducts, the Rivinus ducts, open directly into the floor of the mouth. A large duct, Bartholin duct, may empty into the submandibular duct near its orifice.[7] Primary lymphatic drainage is into level I lymph nodes.

IMAGING WORKUP

MR imaging is the preferred cross-sectional imaging modality to assess a noninflammatory salivary gland mass. Rarely, imaging will be definitive of a diagnosis (**Fig. 3**); however, histologic differentiation of neoplasm is generally not possible on CT or T1-weighted images with or without contrast, although noncontrast T1-weighted images are helpful to assess tumor size, margins, depth, and extent.[8] Certain imaging features may suggest malignancy. Bone invasion, perineural

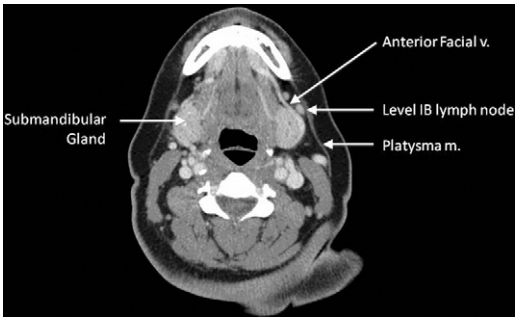

Fig. 2. CT anatomy of the submandibular gland. Whether a mass is glandular or nodal may sometimes be difficult to determine. If the facial vein comes between the gland and the mass, the lesion is nodal.

Fig. 3. Imaging diagnosis of parotid mass. Axial contrast-enhanced CT shows a well-defined fat-density mass within the superficial left parotid gland diagnostic of a lipoma (*arrow*).

spread, and deep extension into the parapharyngeal space or muscles are highly indicative of malignancy. Although infiltrative margins suggest malignancy, hemorrhage or inflammatory changes on CT can create false-positive results for malignancy (**Fig. 4**).

Benign and low-grade malignant lesions are likely to exhibit more hyperintense T2 signal, whereas high-grade malignancies tend to have intermediate or lower T2 signal. T2 signal is influenced by intracellular water content and cellularity. Differentiated benign or low-grade malignant lesions are more likely to produce serous or mucous secretions, which have a high water content. Unfortunately, although elevated T2 signal suggests that a lesion is not high-grade, it does not reliably distinguish between benign and low-grade malignant lesions (**Fig. 5**). Low-grade malignancies, particularly mucoepidermoid and adenoid cystic carcinomas, may exhibit high T2 signal.[9] Some benign lesions can have low T2 signal, including Warthin tumor, which is the second most common benign tumor of the parotid gland, granulomas, and fibrosis. However, for practical purposes, low T2 signal should serve as a warning that a high-grade lesion may be present.[10,11] T1-weighted gadolinium-enhanced fat-saturated sequences should be included to assess for perineural spread, bone invasion, or meningeal involvement if intracranial extension is present. Effacement of fat in the neural foramen on noncontrast T1-weighted images allows for assessment of perineural spread while avoiding artifactual degradation that can be present at the skull base on fat-saturated sequences (**Fig. 6**). Because almost all salivary gland neoplasms enhance, an important role of contrast in assessing the tumor is distinguishing a T2 hyperintense mass from a cyst.

Fig. 4. Inflammatory changes of the parotid gland simulating a malignancy. Axial contrast-enhanced CT demonstrates ill-defined enhancement of the left parotid gland (*arrow*) with areas of low attenuation that represent segments of a dilated intraparotid duct. This focal parotid inflammation could be mistaken for an infiltrative neoplasm. Findings resolved after antibiotics.

MR imaging can delineate the intraparotid course of the facial nerve and parotid ducts. One technique acquires T1-weighted images through a 3-dimensional (3D) Fourier transform gradient-echo sequence (3D GRASS) using a head and neck coil at 1.5 T. Optimal results were obtained with a 20-cm field of view, 512 × 288 matrix, flip angle of 30°, repetition time of 30 ms, and effective echo time of 4.2 ms, and acquiring 60 sections at 1.5-mm thickness without gaps. Facial nerve and intraparotid ducts have lower T1 signal intensity than glandular tissue. Signal intensity within vessels varies with saturation. Curved, orthogonal, and volumetric reconstructed images of the 3D data allow the facial nerve and its branches to be followed in most patients from the stylomastoid foramen through the posterior superior aspect of the gland to the level of the retromandibular vein, and assessment of the parotid ducts at the hilum and in the anteroinferior portion of the gland.[12] This technique is not routine in the authors' practice, because facial nerve branches are each isolated intraoperatively if a local resection is being performed. The course of the nerve is also not relevant if a total parotidectomy is necessary for treatment.

The primary role of fluorodeoxyglucose (FDG) positron emission tomography (PET) is to detect locoregional and distant metastatic disease. The standardized uptake value (SUV) on PET does not reliably distinguish between benign and malignant salivary tumors. Although high-grade tumors tend to have higher FDG uptake than low- or intermediate-grade salivary gland malignancies, benign mixed tumors and Warthin tumors may also have high FDG uptake, resulting in false-positive results (**Fig. 7**). FDG uptake in salivary gland malignancies has also not been shown to be useful in predicting patient survival.[13] Sensitivity of FDG-PET for detecting salivary gland primary malignant tumors has been reported to be between 75% and 100%.[14] False-negative PET results do occur, most frequently in low-grade malignancies wherein lower SUVs may be masked by physiologic FDG uptake in the salivary glands.[13] Studies have shown FDG-PET to be more accurate than conventional imaging

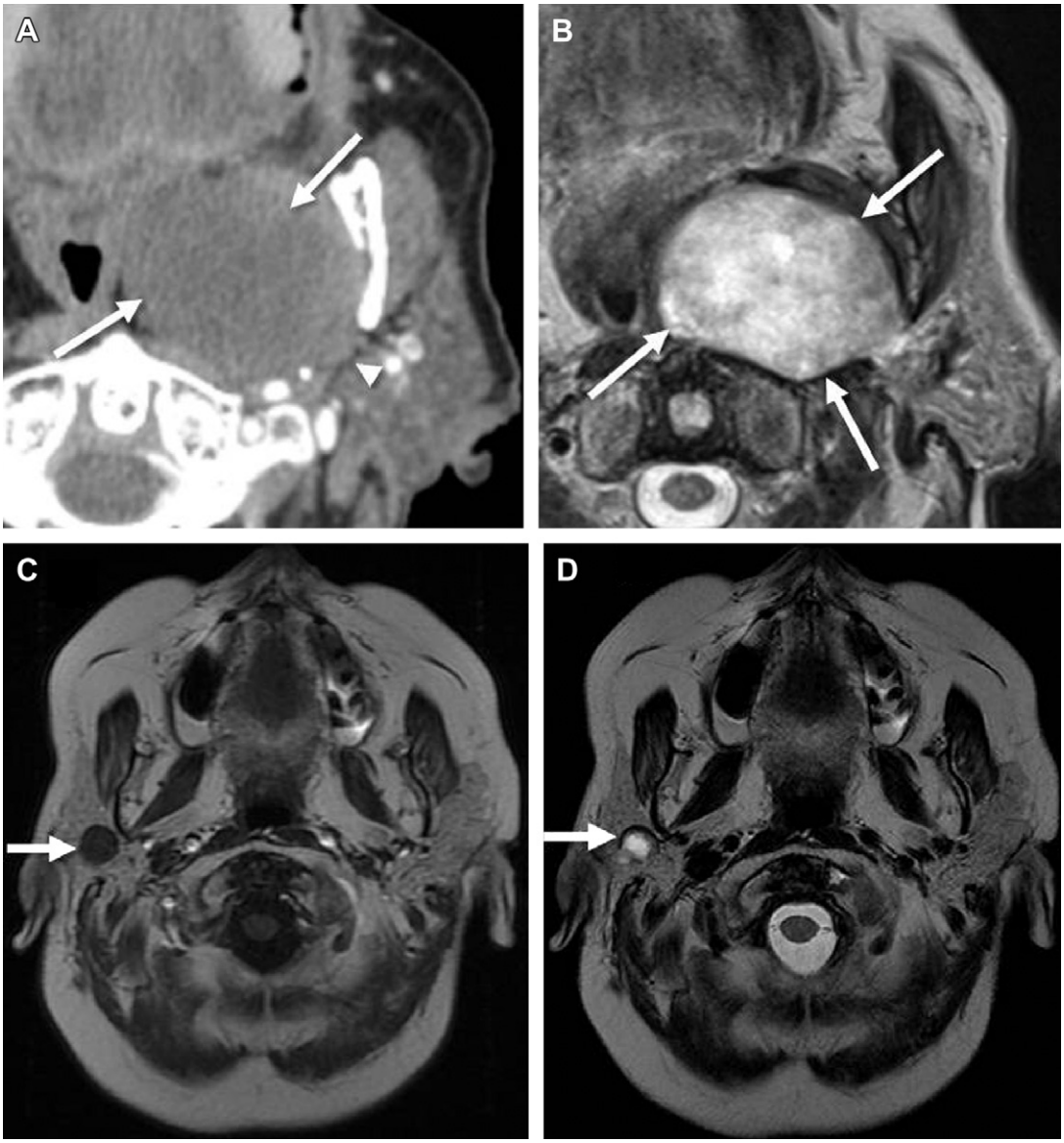

Fig. 5. Overlap in T2 signal intensities in benign and malignant lesions of the parotid gland. (*A*) Axial contrast-enhanced CT shows a well-defined hypodense mass (*arrows*) within the left parapharyngeal space. Note the cleft (*arrowhead*) between deep parotid gland and mass. (*B*) Axial T2-weighted image shows heterogeneous T2 hyperintensity (*arrow*). On surgical resection this was a benign mixed tumor. (*C*) Axial T1-weighted image in a different patient shows a 1.3-cm well-defined low T1 signal mass (*arrow*) in the right parotid gland. (*D*) Axial T2-weighed image shows marked T2 hyperintensity (*arrow*) centrally in this necrotic metastatic lymph node from lung carcinoma.

modalities in detecting locoregional and distant metastatic disease.[14] MR imaging is superior to PET in depicting perineural spread of tumor.

EPIDEMIOLOGY

A painless, enlarging mass in the major salivary glands is most likely caused by a neoplasm, a cyst, or an enlarged lymph node. In general, the rate of malignancy of salivary gland neoplasms is inversely proportional to the gland size. The rate of malignancy is approximately 15% to 32% in the parotid gland, 41% to 45% in the submandibular gland, and 70% to 90% in the sublingual and minor salivary glands.[3]

Cross-sectional imaging of salivary gland neoplasms is typically nonspecific; however, imaging patterns may suggest that a mass is either benign or low-grade malignant, or a higher-grade malignancy. Patterns of disease may help establish a differential diagnosis. Multiple parotid masses

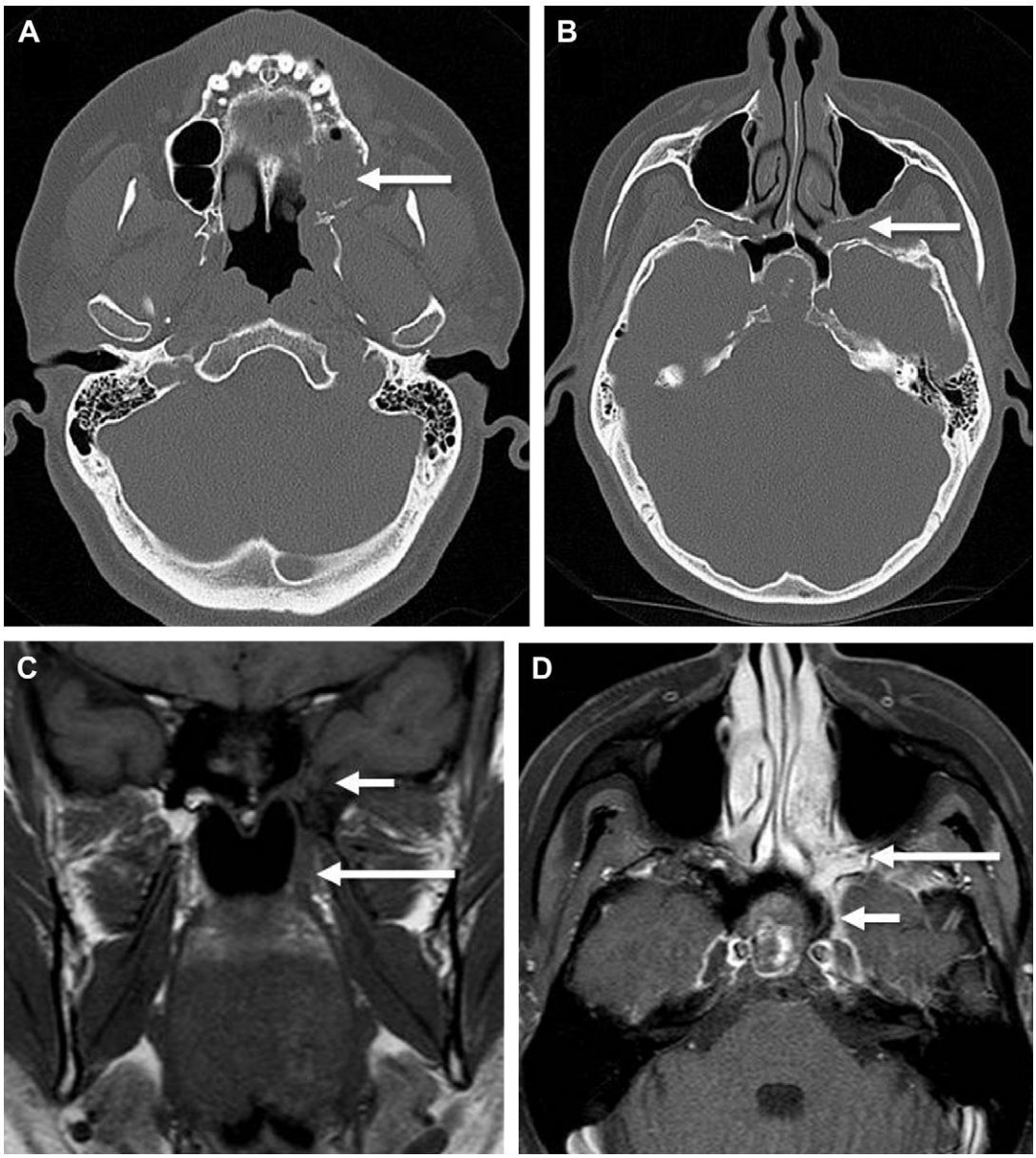

Fig. 6. Perineural tumor extension. (*A*) Axial CT bone windows shows a destructive process (*arrow*) in the left maxillary alveolar ridge in this patient with an adenoid cystic carcinoma of the palate. (*B*) Widening of the left pterygopalatine fossa (PPF) is seen (*arrow*). (*C*) Coronal T1-weighted image shows abnormal T1 hypointense soft tissue replacing the PPF (*long arrow*) and foramen rotundum (*short arrow*). (*D*) Axial postcontrast fat-saturated T1-weighted image confirms abnormal enhancement of the tissue in the PPF (*long arrow*) and foramen rotundum (*short arrow*).

may be from lymphadenopathy, Warthin tumors, Sjögren syndrome, benign lymphoepithelial lesions of HIV, lymphoma, sarcoidosis, or multiple pleomorphic adenomas (usually in the setting of prior surgery or biopsy) (**Fig. 8**).

Benign mixed tumor (BMT), or pleomorphic adenoma, is the most common salivary gland neoplasm, accounting for 60% to 70% of parotid tumors, with approximately 90% arising in the superficial lobe.[7] Pleomorphic adenomas are most commonly well-defined, encapsulated, solitary, T2 hyperintense, enhancing lesions. Larger lesions characteristically assume a lobular contour and are more likely to be heterogeneous in composition. Although no single imaging feature is pathognomonic for BMT, a T2 hyperintense parotid

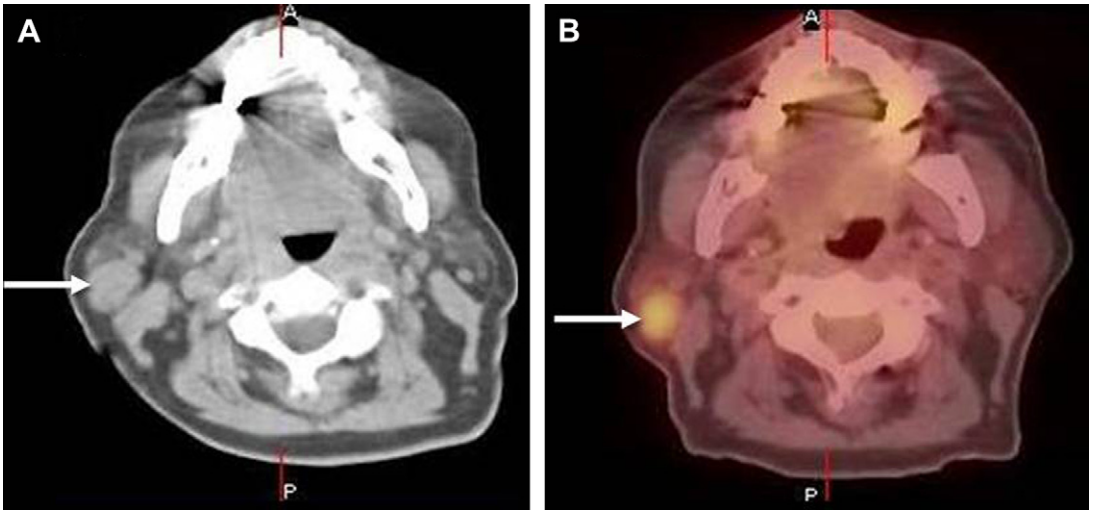

Fig. 7. Elevated FDG uptake in a benign tumor. (*A*) Axial noncontrast CT shows a mass (*arrow*) in the right parotid tail. (*B*) Fused PET-CT image shows hypermetabolism in the mass (*arrow*). On biopsy the mass represented a Warthin tumor.

mass with a complete capsule and lobulated margins is most likely to be a BMT (Fig. 9).[15] Areas of internal hemorrhage, cystic change, or calcification may be present. Dystrophic calcifications, when present, are highly suggestive of BMT.[2] Malignancy may arise in association with primary or recurrent BMT, a risk that increases with tumor duration. Carcinoma ex pleomorphic adenoma (CXPA) accounts for approximately 5% to 15% of all salivary gland malignancies. It has been estimated that malignant degeneration may eventually occur in as many as 25% of untreated BMTs.[16] Imaging features that suggest the possibility of CXPA include areas of low T2 signal and ill-defined infiltrative margins arising within a BMT or in the region of prior resection (Fig. 10). BMT of a deep parotid gland may be clinically silent, so CXPA is a consideration if an unusual or irregular-appearing mass presents in the deep lobe.

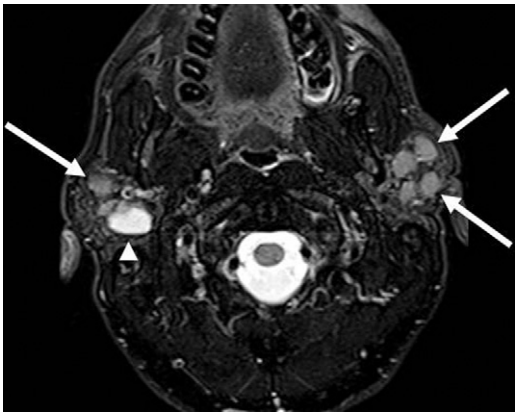

Fig. 8. Pattern of multiple parotid lesions. Axial fat-saturated T2-weighted image in a patient with HIV showing multiple solid (*arrows*) and cystic (*arrowhead*) lesions in both parotid glands, representing benign lymphoepithelial lesions.

Warthin tumor, or papillary cystadenoma lymphomatosum, is the second most common benign tumor of the parotid gland, characteristically located in the tail of the parotid. It is the most common salivary tumor to be bilateral or multifocal. Warthin tumors maintain a well-defined margin and commonly demonstrate cyst formation; however, unlike other benign tumors, areas of low T2 signal are common.[17] Fine-needle aspiration (FNA) may yield thick black cyst contents that are characteristic of Warthin tumors. Furthermore, unlike BMTs, dystrophic calcification is not seen.[2] Other benign epithelial neoplasms of the major salivary glands include basal cell adenoma, oncocytoma, cystadenoma, and myoepithelioma.[3,18] These tumors cannot be reliably distinguished with cross-sectional imaging.

Carcinomas of the major salivary glands are composed of a diverse group of histopathologic entities, including at least 20 different histologic subtypes according to the 2005 WHO classification scheme. This classification distinguishes salivary gland carcinomas from most other head and neck cancers, which are primarily squamous cell carcinomas. According to data compiled by the Armed Forces Institute of Pathology since 1970, the most frequent malignancies of the major salivary glands are mucoepidermoid, acinic cell, adenocarcinoma not otherwise specified (NOS), adenoid cystic carcinoma, and CXPA.

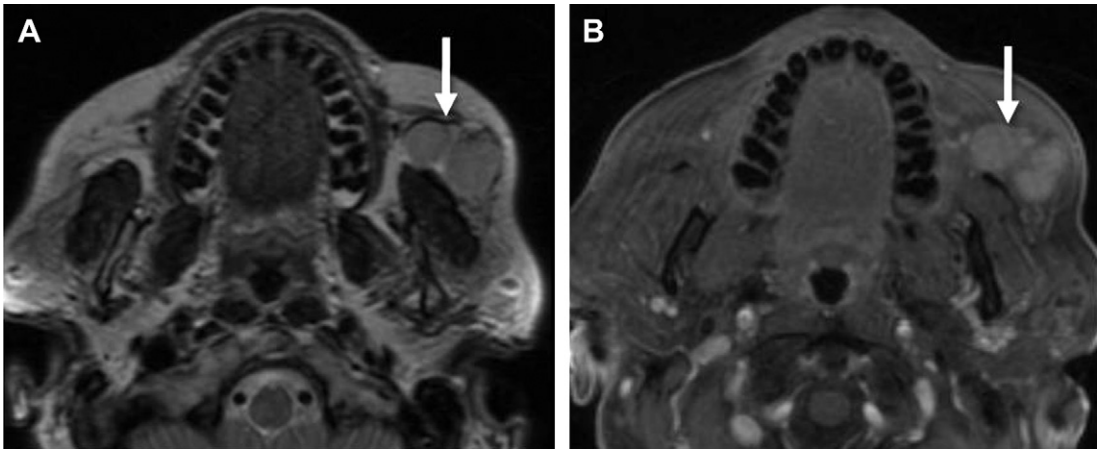

Fig. 9. Benign mixed tumor arising in accessory parotid tissue. (*A*) Axial T2-weighted image shows T2 hyperintensity (*arrow*) in this BMT. (*B*) Axial postcontrast fat-saturated T1-weighted image shows well-defined lobulated enhancing mass (*arrow*) in accessory parotid tissue superficial to the left masseter muscle.

Variability of carcinoma subtypes by demographic parameters has been noted. Squamous cell carcinoma, adenocarcinoma NOS, and salivary ductal carcinoma have higher incidence in men, whereas acinic cell and adenoid cystic carcinoma are higher in women. Except for mucoepidermoid and adenoid cystic carcinoma, which occurred with similar incidence across multiple ethnicities in the United States, all other carcinoma subtypes were more common in Caucasians compared with African Americans, Asians, and Pacific Islanders. All histologic subtypes are more frequent in people older than 50 years.[19] Ionizing radiation is the only well-established risk factor for major salivary gland carcinomas. Additional risk factors, such as viruses, tobacco, alcohol use, ultraviolet light, and occupational exposures, have been suggested to be linked with salivary gland carcinomas.[20] A positive association has been documented between smoking and Warthin tumor.[21]

Given the nonspecific imaging features of salivary malignancies, biopsy or excision is required for diagnosis. Low-grade malignancies, such as mucoepidermoid and acinic cell carcinoma, may be indistinguishable from BMT or other benign tumors on imaging (**Fig. 11**).

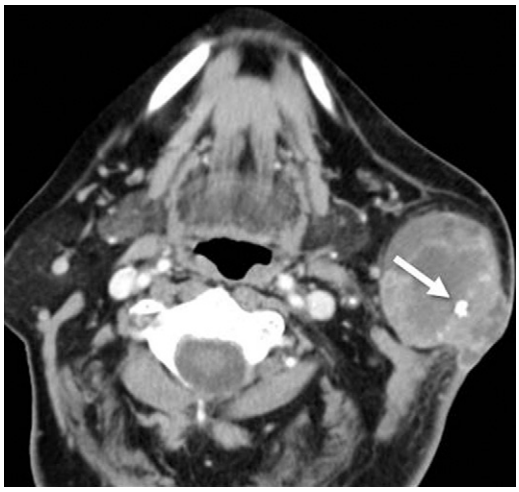

Fig. 10. Carcinoma ex pleomorphic adenoma. Axial contrast-enhanced CT shows a heterogeneously enhancing mass within the superficial left parotid gland. The mass demonstrates well-defined borders except for the posterolateral margin, consistent with extracapsular extension to the skin. A dystrophic calcification is present (*arrow*).

AJCC CANCER STAGING MANUAL, 7TH EDITION: STAGING AND CHANGES FROM PRIOR EDITION

Staging criteria for major salivary gland tumors is unchanged in the 7th edition of the *AJCC Cancer Staging Manual* (*AJCC 7th edition*); however, nomenclature has been slightly adjusted. Several factors related to prognosis and patient survival can be directly assessed radiographically, including location of origin; tumor size; extent of local spread, including facial nerve involvement or perineural extension; and lymph node or distant metastasis.

Primary tumor staging is classified based on size, extraglandular extension, and local invasion (**Tables 1** and **2**). T1 lesions are smaller than 2 cm in diameter. T2 lesions are between 2 and 4 cm in size (**Fig. 12**). T3 lesions constitute tumors

Fig. 11. Overlap in morphology between benign and malignant salivary gland neoplasms. (*A*) Contrast-enhanced CT shows a well-defined predominantly low-attenuation mass (*arrow*) in the left deep parotid lobe that was a surgically confirmed acinic cell carcinoma. (*B*) Contrast-enhanced CT in a different patient shows a similar appearing mass (*arrow*) in the same location that represented a BMT.

larger than 4 cm or those with extraglandular or extraparenchymal extension (Fig. 13). Locally advanced disease (T4 lesions) is stratified into moderately advanced local disease (T4a) and very advanced local disease (T4b). In the *AJCC* 6th edition, T4a and T4b tumors were referred to as resectable and unresectable lesions, respectively. Moderately advanced disease includes tumor that invades the skin (Fig. 14), mandible (Fig. 15), external auditory canal, and/or facial nerve (Fig. 16). Very advanced local disease describes tumor that invades the skull base and/or pterygoid plates, and/or encases the internal carotid artery (Fig. 17).

TRENDS IN TREATMENT AFFECTING STAGING

Preservation of the facial nerve and avoidance of iatrogenic facial nerve injury is a critical concern in planning and performing parotidectomy. Preoperative imaging reports must describe any deep lobe extension of a parotid neoplasm. MR imaging of the parotid region can be performed to demonstrate branches of the facial nerve and their anatomic relationships, but is often not routinely used in clinical practice.

Benign parotid tumors are treated with superficial parotidectomy or, in the case of deep lobe involvement, total parotidectomy with facial nerve dissection and preservation. Wide local margins are preferred, but not always possible if the mass abuts branches of the facial nerve. With optimal surgery, local control for BMT approaches 95%, with low risk of complications. Surgery for locally recurrent disease has an increased risk of complications, particularly facial nerve injury. Postoperative radiotherapy is reserved for patients with positive margins or multifocal recurrent disease.[22] Although superficial parotidectomy is also the preferred treatment for Warthin tumors, enucleation or observation of these benign lesions may be appropriate in select cases.[23]

Treatment of salivary gland malignancies remains primarily surgical excision with wide margins. If possible, the facial nerve is spared during parotid surgery. If the facial nerve must be sacrificed because of direct neural involvement by tumor, immediate reconstruction is usually performed, if possible, using interpositional nerve grafting or segmental reanastamosis.[24] Postoperative radiation therapy is generally indicated in patients with high-grade tumors, or those with locally or regionally advanced disease (T3 or T4), recurrent tumor, or disease at high risk for locoregional recurrence, including perineural or angiolymphatic invasion or extracapsular or extraparotid spread. Neutron beam therapy is also a consideration at some centers.[25] Chemotherapy has a limited role, primarily in palliation of metastatic, recurrent, or advanced unresectable disease.[26]

Nodal spread of disease is more likely to occur with high-grade tumors, although less common than with head and neck mucosal squamous cell carcinomas.[1] Multiple studies have shown N stage to be an independent prognostic factor for survival

Table 1
AJCC 7th edition major salivary glands staging

	Primary Tumor (T)
TX	Primary tumor cannot be assessed
T0	No evidence of primary tumor
T1	Tumor 2 cm or less in greatest dimension without extraparenchymal extension*
T2	Tumor more than 2 cm but not more than 4 cm in greatest dimension without extraparenchymal extension*
T3	Tumor more than 4 cm in greatest dimension and/or tumor having extraparenchymal extension*
T4a	Moderately advanced local disease Tumor invades skin, mandible, ear canal, and/or facial nerve
T4b	Very advanced local disease Tumor invades skull base and/or pterygoid plates and/or encases carotid artery
	* Extraparenchymal extension is clinical or macroscopic evidence of invasion of soft tissues.
	Regional Lymph Nodes (N)
NX	Regional lymph nodes cannot be assessed
N0	No regional lymph node metastasis
N1	Metastasis in a single ipsilateral lymph node, 3 cm or less in greatest dimension
N2	Metastasis in a single ipsilateral lymph node, more than 3 cm but not more than 6 cm in greatest dimension; or in multiple ipsilateral lymph nodes, none more than 6 cm in greatest dimension; or in bilateral or contralateral lymph nodes, none more than 6 cm in greatest dimension
N2a	Metastasis in single ipsilateral lymph node more than 3 cm but not more than 6 cm in greatest dimension
N2b	Metastasis in multiple ipsilateral lymph nodes, none more than 6 cm in greatest dimension
N2c	Metastasis in bilateral or contralateral lymph nodes, none more than 6 cm in greatest dimension
N3	Metastasis in a lymph node more than 6 cm in greatest dimension
	Distant Metastasis (M)
M0	No distant metastasis
M1	Distant metastasis

From Greene FL, Trotti A, Fritz AG, et al, editors. AJCC cancer staging handbook. 7th edition. Chicago: American Joint Committee on Cancer; 2010. Chapter 7: Major Salivary Glands; with permission.

in salivary gland cancer.[27] The rate of lymph node metastasis is positively correlated with the extension of the primary tumor and may be as high as 53% overall.[28] Facial nerve invasion and extraglandular tumor are strongly correlated with an increased risk of nodal metastasis, which imparts a greater than 50% decrease in mean survival.[28]

Lymph node metastasis has been reported to be approximately 7% to 16% in T1 and T2 tumors, with even higher rates reported in other studies.[27] Clinically occult nodal metastases are reported to occur in 8% to 19% of cases.[25] Lymphatic spread tends to be orderly, initially involving intraglandular (parotid) and periglandular nodes, with further dissemination to upper and mid jugular chain nodes (levels II and III), followed by high posterior triangle nodes (level VA). Retropharyngeal spread uncommonly occurs.[1]

Elective neck dissections are usually recommended for high-grade histology or T3 or T4 disease and any patients with evidence of nodal disease regardless of tumor histology.[25] Management of the clinically negative neck (N0) is more controversial. Consequently, some surgeons are more aggressive in pursuing neck dissections in treating major salivary gland cancers, particularly in patients for whom no postoperative radiation therapy is planned.[27]

PATTERNS OF DISEASE SPREAD

All salivary malignancies have the potential for perineural spread, and therefore merit attention

Table 2
Pitfalls in staging of major salivary gland cancers

Pitfall	Advice
Glandular lesion may be isodense on CT	Perform MR imaging with multiple sequences
Benign and malignant neoplasms have similar imaging appearances	FNA has an important role
Perineural tumor extension is common	Know the imaging appearance using pre-contrast T1-weighted images and fat-saturated postcontrast T1-weighted images
Metastatic submandibular lymphadenopathy difficult to differentiate from submandibular gland malignancy	Use course of facial vein to help discern
Noncontiguous involvement of the facial nerve by perineural spread from skip lesions	Evaluate the entire course of the facial nerve for skip lesions

Fig. 12. T2 low-grade mucoepidermoid carcinoma. Axial contrast-enhanced CT shows heterogeneously attenuating 3-cm well-defined right superficial parotid gland mass (*arrow*).

to the skull base for retrograde perineural spread along either cranial nerve VII or the mandibular division of cranial nerve V by way of the auriculotemporal nerve (**Fig. 18**).[29,30] Adenoid cystic carcinoma has a particular tendency toward perineural spread, even with early-stage disease.[31] Imaging findings of perineural spread include widening of neural foramen on CT and thickening of the involved nerves and replacement of fat in the neural foramen on MR imaging. Perineural spread may not always appear contiguous, and skip lesions are possible.

Distant metastases most commonly involve the lungs, followed by osseous structures and the liver. Salivary ductal carcinoma and adenoid cystic carcinoma are the most common histologic types associated with distant metastases. The risk of metastasis is best predicted by tumor size, presence of nodal disease, local extension, and tumor grade. In a retrospective study of 405 patients with major and minor salivary gland malignancies, the reported rate of distant metastases was 11% at 15 years and 24% at 40-year follow-up; 25% of patients developed distant metastases despite apparent local cure.[32]

PITFALLS IN STAGING AND DIAGNOSIS

In addition to the usual descriptions of lesion size, location, and regular or irregular margins, extraparenchymal extension of tumor upstages the mass to T3, and therefore this finding must be reported for parotid and submandibular gland neoplasms because both glands are encapsulated. Irregular border between the tumor and surrounding fibroadipose tissue or frank invasion of surrounding structures are imaging characteristics of extraglandular extension.

Compared with mucosal based lesions of other head and neck subsites, the clinical and imaging presentation of a major or minor salivary gland neoplasm is often nonspecific, with both benign and malignant tumors in the differential. Therefore, preoperative FNA is commonly performed, because both superficial and deep-seated salivary gland masses are amenable to tissue diagnosis using this technique. In fact, the salivary glands are among the most frequently aspirated sites in the head and neck. Tissue biopsy allows nonneoplastic lesions, such as reactive or inflammatory abnormalities, which can be managed medically or expectantly, to be distinguished from benign or malignant neoplastic masses. Biopsy should always be performed with image guidance, because sensitivity for malignancy in blind biopsy of salivary gland masses has been reported to be as low as 38%.[33] Most reports in the literature on

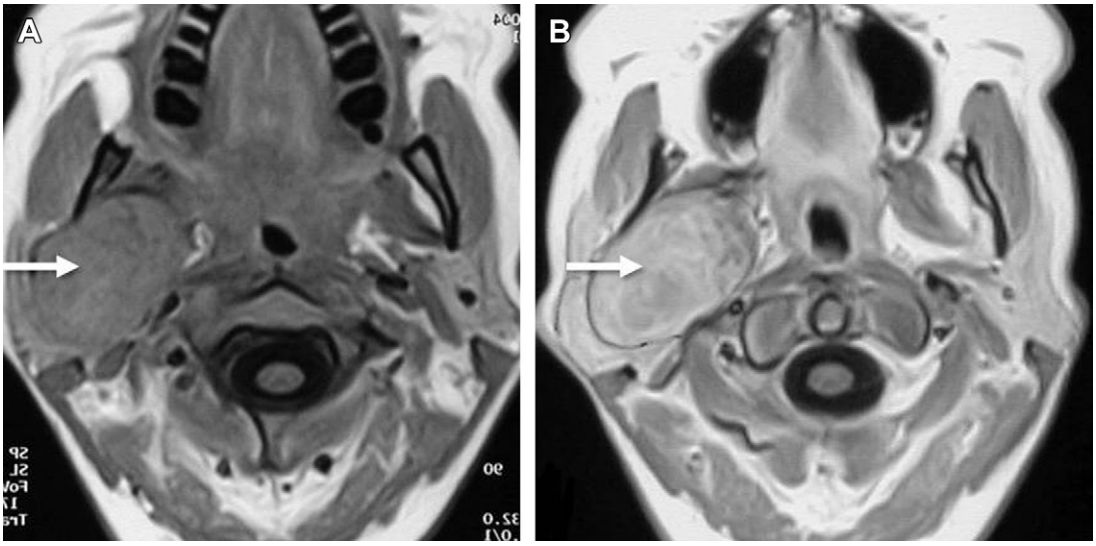

Fig. 13. T3 acinic cell carcinoma. (*A*) Axial T1-weighted image shows a 5-cm well-demarcated right parotid mass (*arrow*). (*B*) Postcontrast T1-weighted image shows fairly homogeneous enhancement in this acinic cell carcinoma (*arrow*).

the safety and efficacy of ultrasound-guided needle diagnosis are limited to the parotid and submandibular glands. This fact may be of little clinical consequence, because neoplastic masses in the sublingual and minor salivary glands are more likely to be malignant.

Tissue effects and complications have been attributed to needle biopsy, including intratumoral hemorrhage, infarction, fibrosis or granulation, and squamous metaplasia.[33] The risk of complication increases with needle size and the number of passes performed. The risk of vascular injury and hematoma is reported to be as high as 1% to 2% after core biopsy.[33] With FNA using a 23- or 25-gauge needle, any tissue effects will be limited in extent and will not hinder correct histopathologic diagnosis.[34]

Fig. 14. Acinic cell carcinoma, T4a from mandibular involvement. Postcontrast fat-saturated T1-weighted image shows an infiltrative mass centered in the deep left parotid gland with destructive changes of the left mandible (*arrow*).

Another criticism of FNA techniques is a higher nondiagnostic or inaccuracy rate with respect to core biopsy. Nondiagnostic or inconclusive samples have been reported to be as high as 18% after FNA.[35] Diagnostic accuracy of FNA can be maximized through onsite cytopathology assessment to confirm specimen adequacy. With appropriate expertise, the diagnostic accuracy of FNA for parotid and submandibular lesions has been reported to be 92%.[33] The nondiagnostic rate is likely to be higher in lesions that are smaller and predominantly cystic. Core needle biopsy has reported accuracy rates up to 97% in diagnosing parotid masses; however, this technique confers a higher risk of complications, such as hemorrhage, facial nerve injury, and seeding of the biopsy tract.[36] In cases showing atypical lymphoid cells on rapid assessment of aspiration samples, specimens should be sent for flow cytometry to evaluate for a monoclonal population characteristic for lymphoma.

The possibility of tumor seeding of the biopsy tract is often mentioned as a potential complication of needle biopsy. Risk of dissemination of neoplastic cells along the biopsy tract is correlated to the size of the needle bore and number of passes made. Additionally, the biopsy tract can be excised with the primary specimen. Clinically detectable tumor cell deposits after FNA are

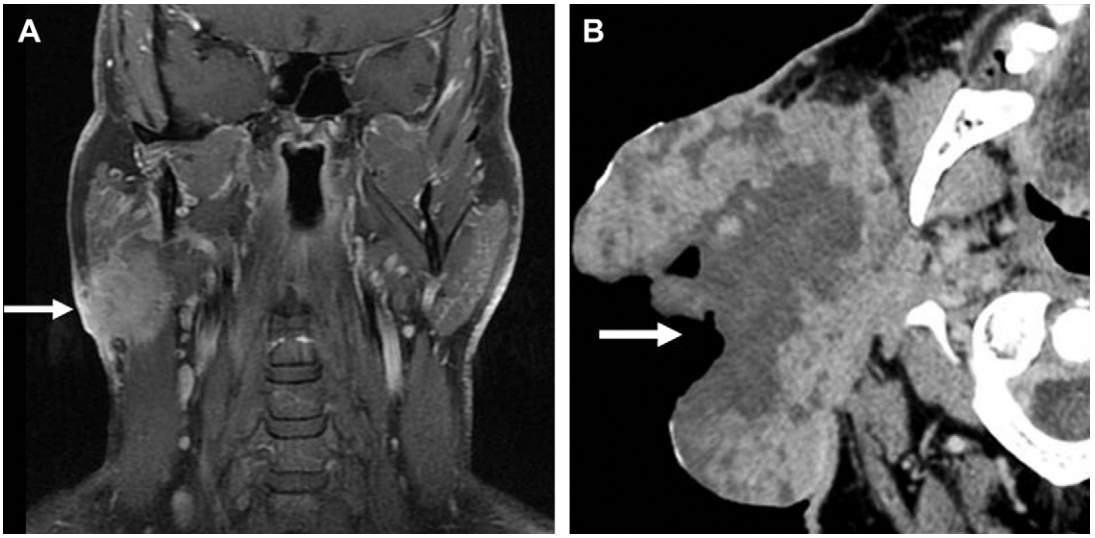

Fig. 15. T4a tumors from skin involvement. (*A*) Coronal postcontrast fat-saturated T1-weighted image shows a right parotid tail mass (*arrow*) that has extended to the skin surface and was visible on physical examination. (*B*) Axial contrast-enhanced CT shows an exophytic and ulcerated mass (*arrow*) in a different patient that has extended to the skin surface extensively.

detected at the skin puncture site in fewer than 0.009% of cases.[37]

Some advantages of FNA for salivary gland lesions are that it helps in preoperative patient counseling, especially with respect to anticipated facial nerve function; treatment planning to determine whether surgery should be urgent or a total gland resection is indicated; diagnosing lesions deemed nonsurgical (eg, lymphoma, inflammatory disease), and determining whether a neck dissection is indicated. However, the decision regarding FNA is surgeon-dependent, and it may not be requested if the mass will be excised regardless of the pathology, or if pathologic support is not available.

SURVEILLANCE PITFALLS AND APPEARANCE OF RECURRENCE

Clinical findings that are concerning for local recurrence of parotid malignancy include a mass or diffuse fullness in the operative bed, and pain in the operative bed or at the skull base. Facial paresis or paralysis in a patient with a history of

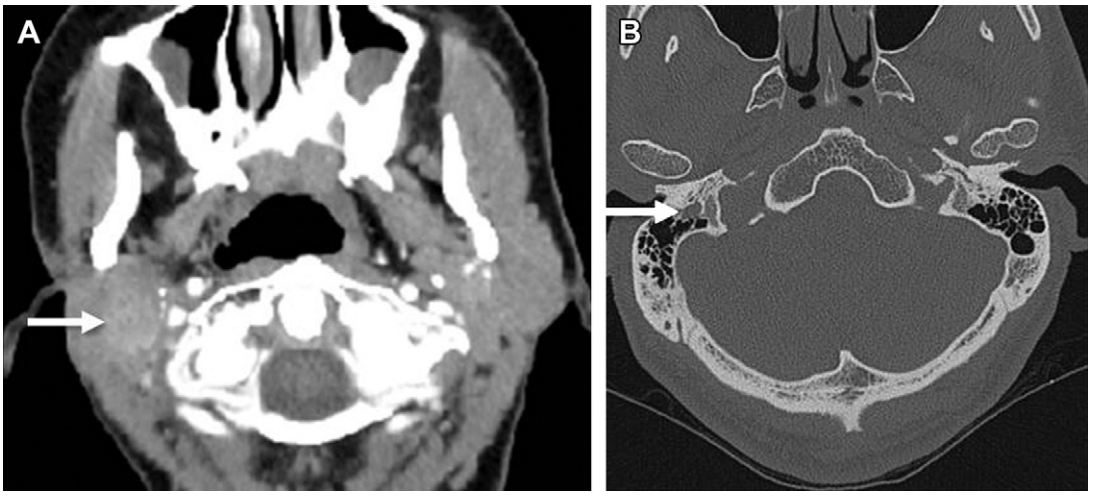

Fig. 16. Poorly differentiated carcinoma of parotid gland, T4a from facial nerve involvement. (*A*) Axial contrast-enhanced CT shows a 2-cm mass (*arrow*) in the right parotid gland with ill-defined margins. (*B*) Bone windows demonstrate enlargement of the right facial nerve canal mastoid segment (*arrow*).

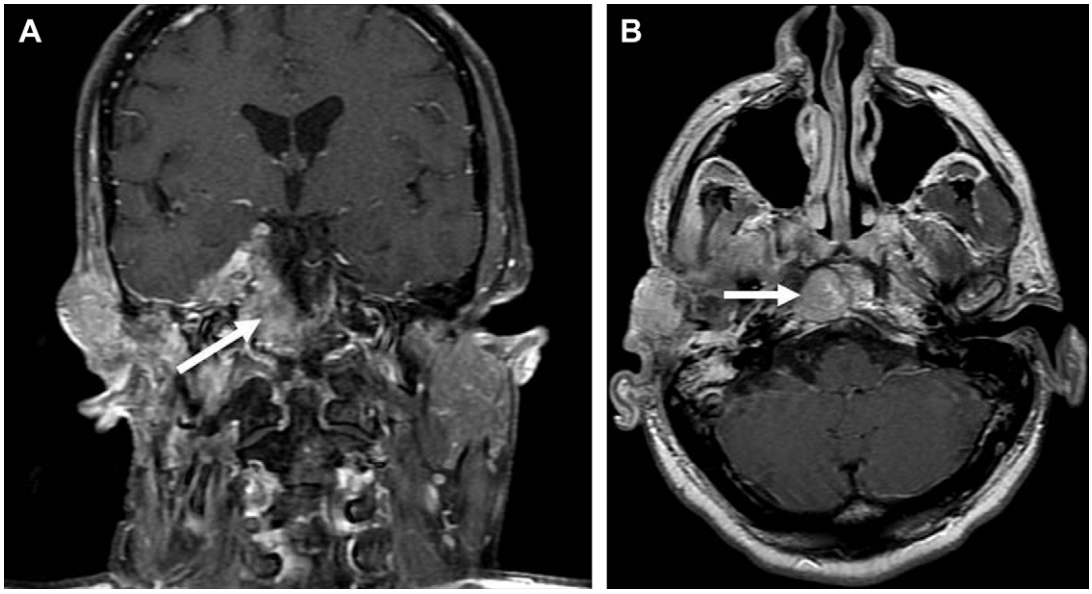

Fig. 17. Acinic cell carcinoma, T4b from skull base involvement. (*A*) Coronal postcontrast fat-saturated T1-weighed image shows extensive masticator space involvement and extension to the skull base (*arrow*) and intracranially. (*B*) Axial postcontrast T1-weighed image with abnormal expansion and enhancement in the clivus (*arrow*).

parotid malignancy must be assumed to reflect recurrent tumor, even in the absence of a clinically detectable mass. Posttreatment otalgia or periauricular pain is concerning for auriculotemporal nerve involvement.

All attempts should be made to obtain preoperative imaging before interpreting postoperative scans. After surgery, non–sharply marginated reactive enhancement and increased T2 signal may be present on MR imaging. These findings

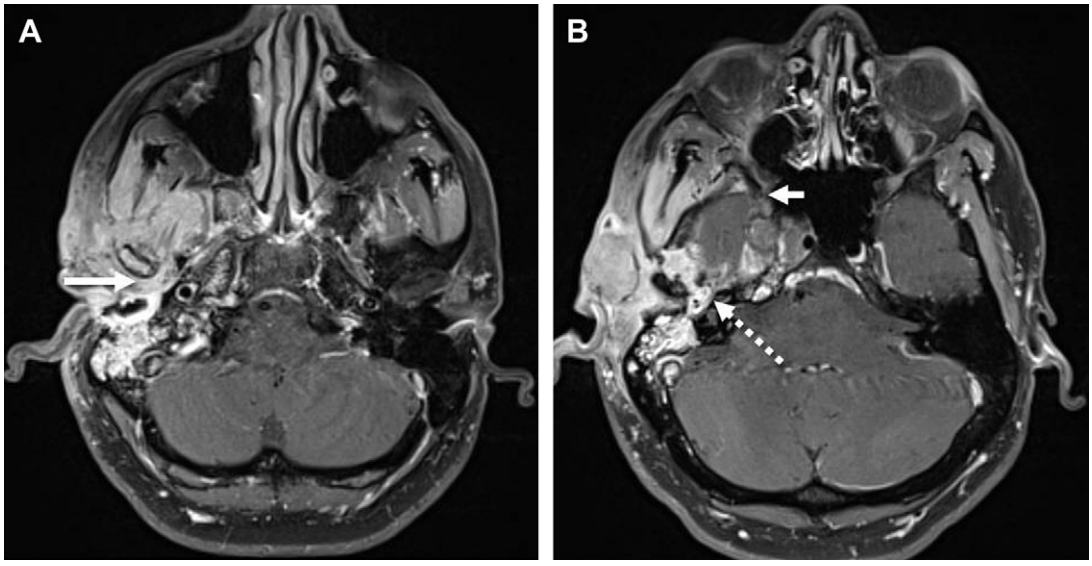

Fig. 18. Auriculotemporal nerve involvement. Axial postcontrast fat-saturated T1-weighed images from a patient with a poorly defined carcinoma. Note abnormal enhancement in the region of the right auriculotemporal nerve (*long arrow*). Perineural tumor extension has occurred along the nerve to V2 and V3 segments of the right trigeminal nerve, with tumor in the right foramen rotundum (*short arrow*) and cavernous sinus, and tumor extension along the facial nerve (*dashed arrow*).

can be misinterpreted as recurrent or residual disease, although in actuality may represent reactive postsurgical changes.[38] The location and appearance of the areas of abnormal signal intensity or attenuation must be correlated with the preoperative appearance of the tumor and the time interval from surgery when deciding whether recurrent or residual disease is likely.

Salivary malignancies may recur along a perineural distribution, especially the facial nerve. Perineural invasion may be present histopathologically, but without radiographically apparent manifestations. In other instances, subtle perineural spread may not have been appreciated on initial staging interpretation. Sialoceles are another possible imaging pitfall after salivary gland surgery (**Fig. 19**). Sialoceles reflect accumulation of secretions after obstruction of intraglandular ducts. Sialoceles appear as a fluid collection with or without rim enhancement. Surrounding enhancement related to postsurgical changes may also be present, complicating the appearance. Sialoceles can be misdiagnosed as abscess or tumor recurrence, particularly when surrounding enhancement or inflammatory changes are present.[38]

FUTURE DIRECTIONS AND ADVANCED IMAGING

Advanced imaging techniques have been advocated as a means to further refine the accuracy of cross-sectional imaging diagnosis. The clinical utility of these techniques is uncertain, because distinguishing whether a neoplasm is benign or low-grade versus high-grade and defining the extent of regional infiltration, perineural spread, and distant metastasis are usually sufficient for the surgeon to plan the operation and counsel the patient about the pertinent risks. Preoperative diagnosis may ultimately be most important in elderly patients and those who are poor surgical candidates, so that unnecessary surgery can be avoided.

Diffusion-weighted imaging with apparent coefficient (ADC) mapping has been used to differentiate benign and malignant salivary gland tumors.[39] Neoplasms with high ADC areas are more likely to be benign. Most malignant tumors had low or very low ADC areas constituting more than 60% of the tumor area. The problem is that this low ADC threshold does not reliably distinguish between malignancies and Warthin tumors. An additional challenge associated with the use of ADC cutoff criteria is that ADC values are affected by the strength of the diffusion gradient applied and vary between MR imaging machines.[37] ADC values can be used to evaluate for areas of malignant change within a pleomorphic adenoma, with low ADC values correlating with the hypercellular carcinomatous portions of the tumor.[40]

Dynamic contrast-enhanced MR imaging has been suggested as a way to differentiate benign from malignant disease, particularly when combined with ADC thresholds. Yabuuchi and

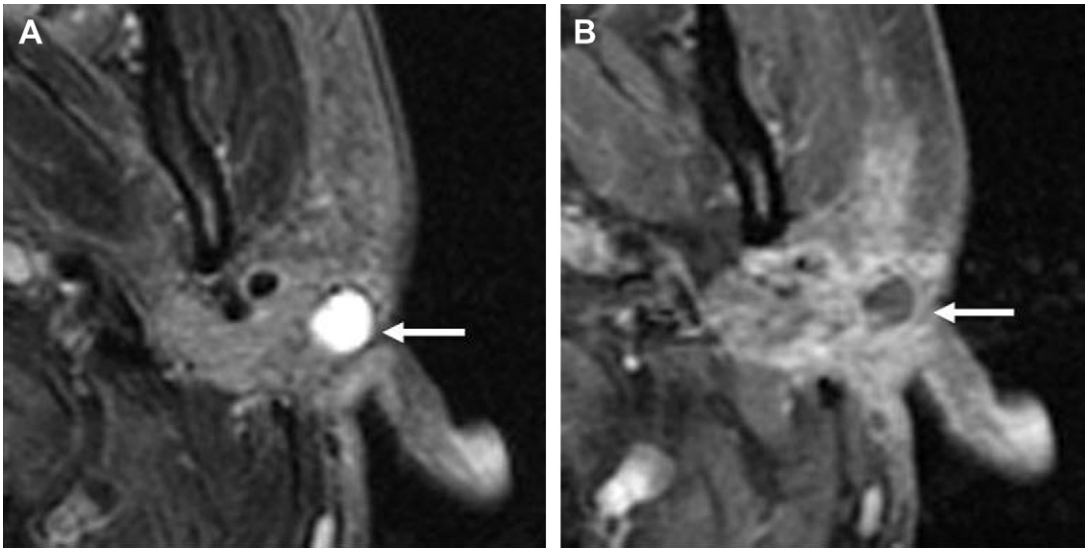

Fig. 19. Postsurgical sialocele mimicking residual tumor. (*A*) Axial T2-weighed image shows a well-defined markedly T2 hyperintense collection (*arrow*) in the postoperative bed after left superficial parotidectomy. (*B*) Axial postcontrast fat-saturated T1-weighed image shows nonenhancement of the area with expected surrounding postoperative changes (*arrows*); this should not be mistaken for an abscess or residual/recurrent tumor. (*Courtesy of* L. Ginsberg, MD, Anderson Cancer Center, Houston, Texas.)

colleagues[41] classified time-signal intensity curves (TIC) into 4 patterns of enhancement based on the time of peak enhancement and washout ratio. Type A (persistent pattern) shows gradual enhancement with a time to peak of longer than 120 seconds. Type B (washout pattern) has a shorter time to peak ($\leq$120 seconds) with a washout ratio of greater than 30%. Type C (plateau pattern) has a time to peak equal or less than 120 seconds and a washout ratio of less than 30%. Type D is a flat pattern, typical of predominantly cystic tumors. Histopathologically, the time to peak correlates with microvessel count, a marker for tumor vascularity, and washout ratio reflects the cellular-stromal grade of the tumor. A larger extracellular space with fibrous stromata retains contrast longer, so carcinomas that have a low cellularity-stromal grade will have a low contrast washout ratio. The persistent and flat curves show high sensitivity and specificity for benign disease. A washout curve is also typical for benign disease but not completely specific. Certain malignancies, such as acinic cell carcinoma, have a washout type TIC. A plateau curve is sensitive but demonstrates suboptimal specificity for malignant disease. Adding ADC cutoff values to tumors that demonstrate a washout or plateau TIC pattern has been proposed as a means to improve specificity in predicting benignity versus malignancy of a tumor.[42]

Proton MR spectroscopy has been evaluated for its ability to characterize salivary gland tumors, but currently has limited clinical applicability. Spectra obtained from normal parotid glands demonstrate lipids but no detectable choline (Cho) or creatine (Cr) peaks. Elevated choline, a marker of cell membrane turnover, is found in both benign and malignant tumors. An early study by King and colleagues[43] found an echo time of 136 ms to be the most successful to obtain a Cr peak for calculation of a Cho/Cr ratio. In their study, a Cho/Cr ratio greater than 2.4 had 100% positive predictive value that a salivary gland tumor was benign. Warthin tumor was likely to have a Cho/Cr ratio more than 4.5, possibly because of the larger number of lymphocytes in these tumors.

SUMMARY

Most neoplasms in other subsites in the head and neck are squamous cell carcinoma, but tumors of the salivary glands may be benign or malignant. Surgical treatment differs if the lesion is benign, and therefore preoperative FNA is important in salivary neoplasms. The role of imaging is to attempt to determine histology, predict likelihood of a lesion being malignant, and report an imaging stage. Staging is based on size for T1 through T3 lesions and whether extraglandular extension is present. Involvement of the skull base or pterygoid plates, or the presence of pericarotid disease, upstages the lesion to T4b and must be mentioned in the radiology report.

REFERENCES

1. Greene FL, Trotti A, Fritz AG, et al, editors. AJCC cancer staging handbook. 7th edition. Chicago: American Joint Committee on Cancer; 2010.
2. Som PM, Brandwein-Gensler MS. Anatomy and pathology of the salivary glands. In: Som PM, Curtain HD, editors. Head and neck imaging. 5th edition. St Louis (MO): Elsevier Mosby; 2011. p. 2449–609.
3. Ellis GL, Auclair PL. Tumors of the salivary glands. Washington, DC: Armed Forces Institute of Pathology; 2008.
4. Standring S, editor. Grays anatomy: the anatomical base of clinical medicine. 39th edition. Edinburgh (Scotland): Elsevier Churchill Livingstone; 2005. p. 515–7, 602–4.
5. McKean ME, Lee K, McGregor IA. The distribution of lymph nodes in and around the parotid gland: an anatomical study. Br J Plast Surg 1985;38:1–5.
6. Weissman JL, Carrau RL. Anterior facial vein and submandibular gland together: Predicting the histology of submandibular masses with CT or MR imaging. Radiol 1998;208:441–6.
7. Gnepp DR, Brandwein MS, Henley JD. Salivary and lacrimal glands. In: Gnepp DR, editor. Diagnostic surgical pathology of the head and neck. 1st edition. Philadelphia: W.B. Saunders Company; 2001. p. 325–430.
8. Yousem DM, Kraut MA, Chalian AA. Major salivary gland imaging. Radiol 2000;216:19–29.
9. Sigal R, Monnet O, de Baere T, et al. Adenoid cystic carcinoma of the head and neck: evaluation with MR imaging and clinical-pathologic correlation in 27 patients. Radiology 1992;184:95–101.
10. Som PM, Biller HF. High-grade malignancies of the parotid gland: identification with MR imaging. Radiol 1989;173:823–6.
11. Christe A, Waldherr C, Hallett R, et al. MR imaging of parotid tumors: typical lesion characteristics in MR imaging improve discrimination between benign and malignant disease. AJNR Am J Neuroradiol 2011;32(7):1202–7.
12. Dailiana T, Chakeres D, Schmalbrock P, et al. High-resolution MR of the intraparotid facial nerve and parotid duct. AJNR Am J Neuroradiol 1997;18: 165–72.
13. Roh JL, Ryu CH, Choi SH, et al. Clinical utility of 18F-FDG PET for patients with salivary gland malignancies. J Nucl Med 2007;48:240–6.

14. Cermik TF, Mavi A, Acikgoz G, et al. FDG PET in detecting primary and recurrent malignant salivary gland tumors. Clin Nucl Med 2007;32:286–91.
15. Ikeda K, Katoh T, Ha-Kawa SK, et al. The usefulness of MR in establishing the diagnosis of parotid pleomorphic adenoma. AJNR Am J Neuroradiol 1996; 17:555–9.
16. Lewis JE, Olsen KD, Sebo TJ. Carcinoma ex pleomorphic adenoma: pathologic analysis of 73 cases. Hum Pathol 2001;32:596–604.
17. Ikeda M, Motoori K, Hanazawa T, et al. Warthin tumor of the parotid gland: diagnostic value of MR imaging with histopathologic correlation. AJNR Am J Neuroradiol 2004;25:1256–62.
18. Weinstein GS, Harvey RT, Zimmer W, et al. Technetium-99m pertechnetate salivary gland imaging: Its role in diagnosis of Warthin's tumor. J Nucl Med 1994;35:179–83.
19. Boukheris H, Curtis RE, Land CE, et al. Incidence of carcinoma of the major salivary glands according to the WHO classification, 1002 to 2006: a population-based study in the United States. Cancer Epidemiol Biomarkers Prev 2009;18:2899–906.
20. Horn-Ross PL, Ljung B, Morrow M. Environmental factors and the risk of salivary gland cancer. Epidemiology 1997;8:414–9.
21. Kotwall CA. Smoking as an etiologic factor in the development of Warthin's tumor of the parotid gland. Am J Surg 1992;164:646–7.
22. Mendenhall WM, Mendenhall CM, Werning JW, et al. Salivary gland pleomorphic adenoma. Am J Clin Oncol 2008;31:95–9.
23. Yoo GH, Eisele DW, Askin FB, et al. Warthin's tumor: a 40-year experience at The Johns Hopkins Hospital. Laryngoscope 1994;104:799–803.
24. Scianna JM, Petruzelli GJ. Contemporary management of tumors of the salivary glands. Curr Oncol Rep 2007;9:134–8.
25. Bell RB, Dierks EJ, Homer L, et al. Management and outcome of patients with malignant salivary gland tumors. J Oral Maxillofac Surg 2005;63:917–28.
26. Day TA, Deveikis J, Gillespie MB, et al. Salivary gland neoplasms. Curr Treatment Opin Oncol 2004;5:11–26.
27. Stennert E, Kisner D, Jungehuelsing M, et al. High incidence of lymph node metastasis in major salivary gland cancer. Arch Otolaryngol Head Neck Surg 2003;129:720–3.
28. Bhattacharyya N, Fried MP. Nodal metastasis in major salivary gland cancer. Arch Otolaryngol Head Neck Surg 2002;128:904–8.
29. Schmalfuss IM, Tart RP, Jukherji S, et al. Perineural tumor spread along the auriculotemporal nerve. Am J Neuroradiol 2002;23:303–11.
30. Ginsberg LE. Imaging of perineural tumor spread in head and neck cancer. Semin Ultrasound CT MRI 1999;20:175–86.
31. Bradley PJ. Adenoid cystic carcinoma of the head and neck: a review. Curr Opin Otolaryngol Head Neck Surg 2004;12:127–32.
32. Bradley PJ. Distant metastases from salivary glands cancer. ORL J Otorhinolaryngol Relat Spec 2001;63: 233–42.
33. Sharma G, Jung AS, Maceri DR, et al. US-guided fine-needle aspiration of major salivary gland masses and adjacent lymph nodes: accuracy and impact on clinical decision making. Radiol 2011; 259:471–8.
34. Mukunyadzi P, Bardales RH, Palmer HE, et al. Tissue effects of salivary gland fine-needle aspiration. Does this procedure preclude accurate histologic diagnosis? Anat Pathol 2000;114:741–5.
35. Cajulis RS, Gokaslan ST, Yu GH, et al. Fine needle aspiration biopsy of the salivary glands: a five-year experience with emphasis on diagnostic pitfalls. Acta Cytol 1997;41:1412–20.
36. Wan YL, Chan SC, Chen YL, et al. Ultrasonography-guided core-needle biopsy of parotid gland masses. AJNR Am J Neuroradiol 2004;25:1608–12.
37. Supriya M, Denholm S, Palmer T. Seeding of tumor cells after fine needle aspiration cytology in benign parotid tumor: a case report and literature review. Laryngoscope 2008;118:263–5.
38. Ginsberg LE. Imaging pitfalls in the postoperative head and neck. Semin Ultrasound CT MRI 2002; 23:444–59.
39. Eida S, Sumi M, Sakihama N, et al. Apparent diffusion coefficient mapping of salivary gland tumors: prediction of the benignancy and malignancy. AJNR Am J Neuroradiol 2007;28:116–21.
40. Kato H, Kanematsu M, Mizuta K, et al. Carcinoma ex pleomorphic adenoma of the parotid gland: radiographic-pathologic correlation with MR imaging including diffusion-weighted imaging. AJNR Am J Neuroradiol 2008;29:865–7.
41. Yabuuchi H, Fukuya T, Tajima T, et al. Salivary gland tumors: diagnostic value of gadolinium-enhanced dynamic MR imaging with histopathologic correlation. Radiol 2003;226:345–54.
42. Yabuuchi H, Matsuo Y, Kamitani T, et al. Parotid gland tumors: can addition of diffusion-weighted MR imaging to dynamic contrast-enhanced MR imaging improve diagnostic accuracy in characterization? Radiol 2008;249:909–16.
43. King AD, Yeung DK, Ahuja AT, et al. Salivary gland tumors at in vivo proton MR spectroscopy. Radiol 2005;237:563–9.